Roberts, Hannah ; Pichler, Thomas

Hg in the hydrothermal fluids and gases in Baia di Levante, Vulcano, Italy

Journal Article as: peer-reviewed accepted version (Postprint)

DOI of this document*(secondary publication): https://doi.org/10.26092/elib/3127

Publication date of this document: 02/12/2024

* for better findability or for reliable citation

Recommended Citation (primary publication/Version of Record) incl. DOI:

Roberts, Hannah ; Pichler, Thomas. 2022. Hg in the hydrothermal fluids and gases in Baia di Levante, Vulcano, Italy. Marine Chemistry, vol. 244. © Elsevier. DOI: 10.1016/j.marchem.2022.104147.

Hg in the hydrothermal fluids and gases in Baia di Levante, Vulcano, Italy

Hannah Roberts *, Thomas Pichler

Universität Bremen, Fachbereich Geowissenschaften, Geochemistry and Hydrogeology, Klagenfurter Str. 2-4, 28359 Bremen, Germany

A B S T R A C T

The importance of fluid and gaseous mercury (Hg) emissions from hydrothermal systems in the shallow, coastal ocean is poorly constrained. However, there are indicators that they could be a significant natural Hg source. We evaluated the hydrothermal Hg emissions around Vulcano Island, Aeolian Arc, Italy, which is host to a marine shallow-water hydrothermal system (MSWHS) in Baia di Levante. Fluids were collected with porewater probes, and gases were collected into Tedlar© bags. Total Hg (THg) concentrations in the hydrothermal fluids ranged from 2.9 to 2888 pM. The concentrations of volatile Hg were below 8 pM and trended positively with increasing temperature. Monomethyl Hg (MMHg) was not detected. Total Hg in the gases ranged from 0.03 to 1.82 μmol/m^3.

High concentrations of THg were associated with low Cl-concentrations, low pH-values, and high K/Cl and Mg/Cl ratios. Concentrations of THg in the hydrothermal fluids resulted from mixing between meteoric water, seawater, condensed fumarolic vapor, and a deep hydrothermal fluid. However, not all low-Cl fluids were high THg samples. Samples taken along the coast of the La Fossa crater contained substantially less THg (2.9 to 29.4 pM), despite similar hydrothermal indicators as those in the Baia di Levante samples. These data support subsurface circulation models, which discuss the downslope flow of condensed La Fossa crater gases to the coast. In the hydrothermally active area of Baia di Levante, concentrations of THg were elevated relative to background surface seawater, ranging from 40 to 5110 pM. In comparison, the remainder of the bay ranged from 0.8 to 2.4 pM.

The flux of Hg to the atmosphere from surface waters was calculated through dissolved Hg concentrations. The flux at each sampled site ranged from 0 to 19.6 pmol/$m^{2/}$hr. The highest flux rates were determined for those areas with visible hydrothermal activity, particularly those with high gaseous emission rates. Surface water concentrations declined rapidly away from point sources, indicating atmospheric emission, dilution through mixing, or scavenging and sedimentation. In hydrothermally active areas, Baia di Levante sediments contained THg concentrations of 2.42 nmol/g and 49.52 nmol/g, which were significantly above background (0.03 nmol/g).

The largest gaseous point source, Bambino, released >2 L of gas per second. Although, Hg concentrations in the gas were low (113 to 122 nmol/m^3) relative to other measured point sources near the beach (1768 to 1817 nmol/m^3), due to the volume of discharge, surface water concentrations were elevated (131 pM).

The Hg present in the hydrothermal system of Vulcano contributes Hg to the atmosphere and local seawater as a natural source.

1. Introduction

Mercury (Hg) is a well-known biological toxin affecting environmental and human health. Anthropogenic Hg emissions are the primary source to the environment, while natural sources of Hg play a lesser role and are poorly constrained in global models (Lamborg et al., 2002; Outridge et al., 2018). In the marine cycle, Hg is primarily deposited from the atmosphere to surface waters as elemental Hg (Hg^0) or ionic Hg (Hg^{2+}) (Mason and Fitzgerald, 1996; Mason and Sheu, 2002). Abiotic and biotic reactions oxidize Hg^0 to ionic Hg (Hg^{2+}), after which primarily biological processes generate methylated species monomethylmercury and dimethylmercury (MMHg and DMHg) (Fitzgerald et al., 2007). These organic Hg compounds are highly toxic, given their ability to pass through the blood-brain barrier. Additionally, organic

* Corresponding author.
E-mail address: roberts@uni-bremen.de (H. Roberts).

species bioaccumulate to levels that can affect human health. Dissolved species (Hg_{diss}) include colloidally bound Hg (< 0.45 μm) and unbound Hg^{2+}, Hg^0, and methylated species. Volatile species include Hg^0 and DMHg. Total Hg (THg), which includes dissolved and particle-bound Hg, in the Mediterranean Sea, is generally in the low pM (< 5 pM) concentration range with variable concentrations in the water column spatially and temporally (e.g., Cossa et al., 2018; Cossa et al., 1997b; Fitzgerald et al., 2007; Horvat et al., 2003).

Marine shallow-water hydrothermal systems (MSWHS) are sparingly described natural sources of Hg to the atmosphere and marine environment (e.g., Bagnato et al., 2017; Leal-Acosta et al., 2010; Roberts et al., 2021; Stoffers et al., 1999). Emission types can be concentrated at a single point (point sources) or occur diffusely across a wide area (diffusive flux) and are generally associated with elevated temperatures of up to 120 °C (Pichler et al., 1999b; Price and Giovannelli, 2017; Roberts et al., 2021). Features associated with MSWHS include microbial mats (e.g., Price and Giovannelli, 2017; Price et al., 2013b); chimneys and hydrothermal precipitates (e.g., Esposito et al., 2018; Pichler and Veizer, 2004); and fluid, brine, and gas emission (e.g., Bagnato et al., 2009; Pichler et al., 1999a; Valsami-Jones et al., 2005). As a volatile element, Hg can be present in hydrothermal systems in the gas or fluid phase (Roberts et al., 2021; Varekamp and Buseck, 1984). Depending upon depth and gas flow, emissions from MSWHS can contribute Hg directly to the atmosphere or dissolve constituents into the water column (e.g., Bagnato et al., 2017; Pichler et al., 1999a; Pichler et al., 1999c; Roberts et al., 2021). At the point of emission, no methylated species have been observed in fluids from MSWHS (Roberts et al., 2021). However, contributions of inorganic Hg species to local waters, seagrasses, and sediments have been reported (Bagnato et al., 2017; Leal-Acosta et al., 2013; Leal-Acosta et al., 2010; Roberts et al., 2021). Additionally, the methylation of inorganic species within the water column is a significant factor within the marine Hg cycle (Lehnherr et al., 2011; Monperrus et al., 2007; Munson et al., 2018).

Here, we present Hg and water chemistry data for the hydrothermal

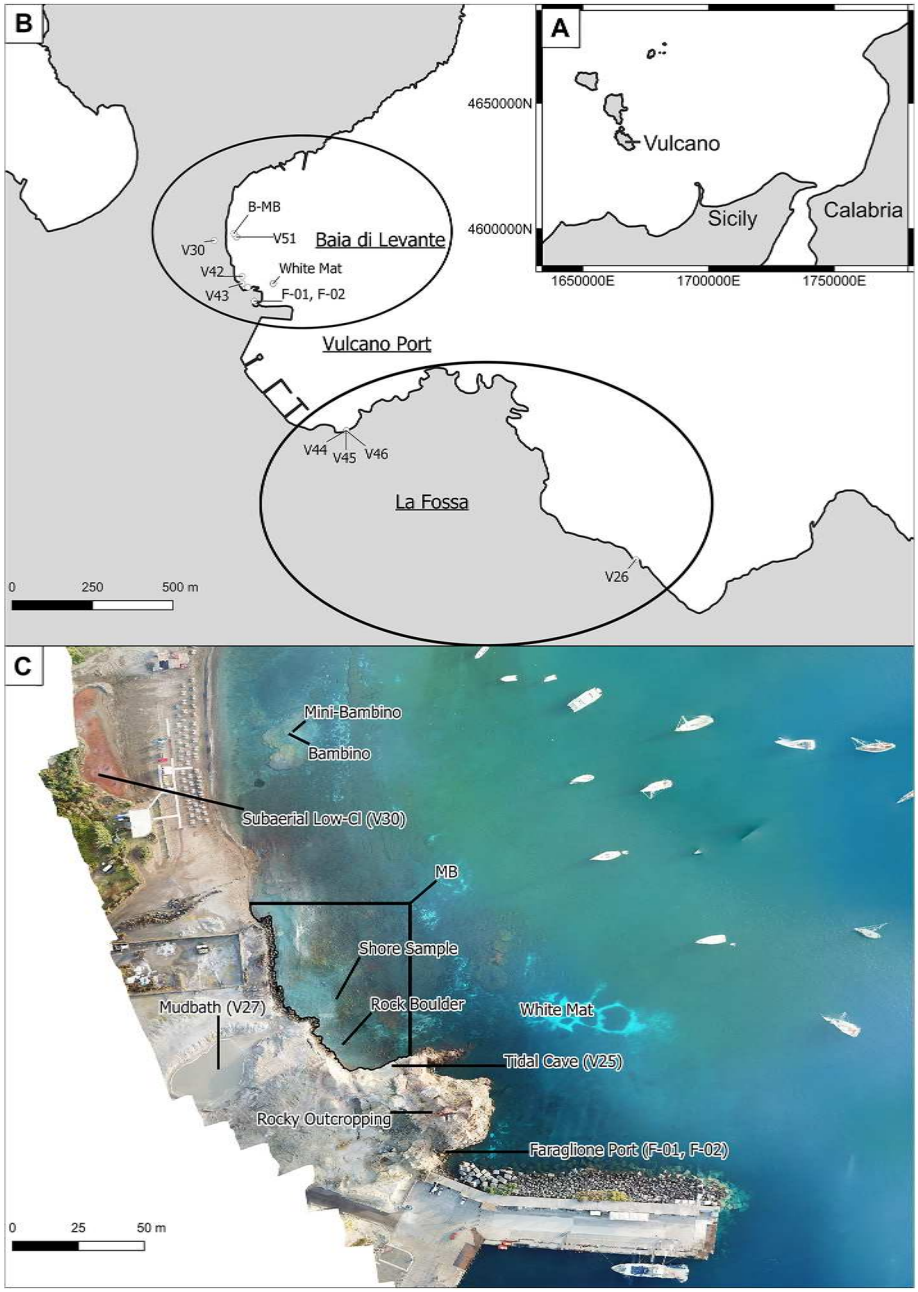

Fig. 1. Map of all hydrothermal sample locations on Vulcano island with A) regional map, B) map of Baia di Levante and the La Fossa samples with locations of hydrothermal samples. LF samples were distinctive from Baia di Levante samples with greater influence from the La Fossa crater. The maps were generated in QGIS. C) Map of Baia de Levante hydrothermally active area showing named point sources including subaerial low-Cl, shore, rock boulder, tidal cave, Bambino, white mat, and the mud bath area (MB). Created from drone images that were stitched with Microsoft ICE.

fluids and gases of the Vulcano MSWHS, along with data for surface waters in Baia di Levante (Fig. 1). We hypothesize the source of Hg to be a rising hydrothermal vapor phase. The final concentration of Hg is controlled by mixing seawater and meteoric water. These findings support previous studies of subsurface circulation models (Oliveri et al., 2019; Zambardi et al., 2009) and groundwater studies (Aiuppa et al., 2000; Bagnato et al., 2009).

2. Geological setting

The island of Vulcano belongs to the Aeolian volcanic arc and is comprised entirely of volcanic rock, with younger volcanic edifices in the north and northwest (Keller, 1980). Volcanic activity began during the Upper Pleistocene, and the last eruptive period was from 1888 to 1890; however variable fumarolic activity on land and offshore has continued to the present (De Astis et al., 1997). Baia di Levante is located between the La Fossa caldera and the Vulcanello peninsula. Following drilling campaigns in the 1950s, the Baia di Levante area has been known to be fed by a hydrothermal aquifer beneath the bay (Sommaruga, 1984). Since that time, several subsurface circulation models have been proposed (e.g., Aiuppa et al., 2020; Falcone et al., 2022; Federico et al., 2010; Fulignati et al., 1998; Inguaggiato et al., 2012; Madonia et al., 2015; Oliveri et al., 2019). All models agree that the system is driven by a shallow geothermal aquifer, which generates a boiling hydrothermal brine that feeds the MSWHS in Baia di Levante. However, the exact subsurface plumbing of the hydrothermal aquifer, the sources of various marine and sub-aerial point sources, and the relative significance of water sources (e.g., meteoric water and seawater) are not conclusively established. Large variations in gas and liquid composition and temperature were reported for the La Fossa and Baia di Levante areas (e.g., Aiuppa et al., 2007; Aubert et al., 2008; Boatta et al., 2013; Rogers et al., 2007). In Baia di Levante, multiple shallow-water point sources emit metals, REEs, and other components to the seawater, which affect the water chemistry of the bay (e.g., Capaccioni et al., 2001; Oliveri et al., 2019; Sedwick and Stuben, 1996).

Hydrothermal activity is present north of the Vulcano port along the beach and in the shallow bay (Figs. 1 and 2). Activity in the bay was observed primarily in the form of gaseous exhalations. An area of diffuse hydrothermal fluid flux is indicated by the formation of white biomats north of the port (Fig. 1). A large, acidic mud bath frequented by tourists sits to the west of the bay, immediately onshore and north of the port. The rocky outcropping that divides the beach and port areas contains at least three acidic hydrothermal sources below or above sea level. The area in Baia di Levante north of the outcropping area and directly east of the mud bath is considered the mud bath area (MB) for purposes of data discussion. North of MB is the largest gaseous exhalation in the bay, named Bambino. Eastward from Bambino are many small gaseous exhalations in addition to a point source northeast of Bambino (Mini-

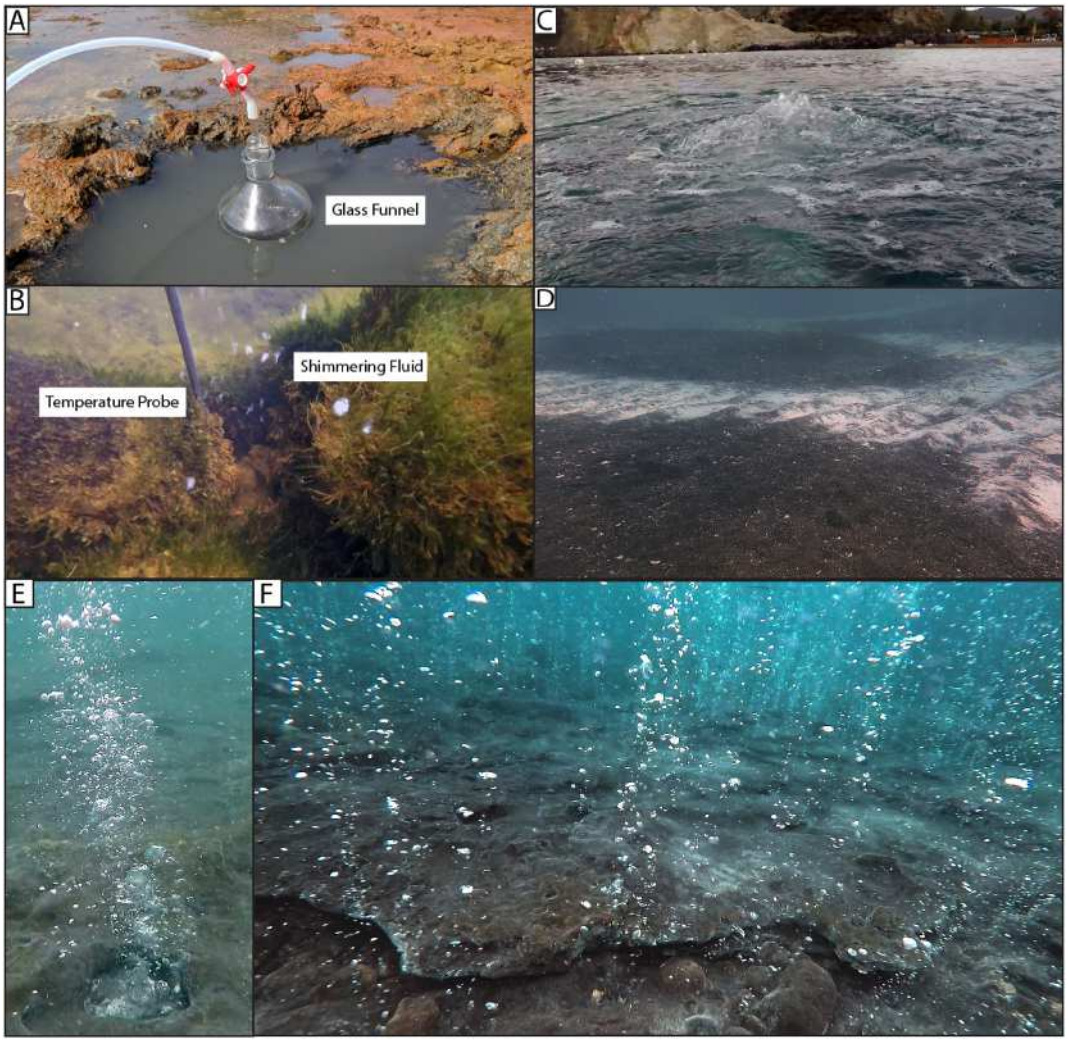

Fig. 2. Point source examples on Vulcano island. A) gas sampling of subaerial low-Cl, B) submarine low-Cl with shimmering hydrothermal fluid, C) Bambino surface emission, D) white mat area. Point sources in the area of Bambino E) gaseous point source (Mini-Bambino), F) extensive gaseous exhalations to the east of Bambino.

Bambino). Between the rocky outcropping and Bambino, the bottom substrate is rocky with little sedimentation close to shore. Waters are often murky, with large flocculants visible in the water column. The area to the north of Bambino contains only a few small gaseous point sources (Aiuppa et al., 2020; Boatta et al., 2013). Small, low-Cl point sources emit gas and fluid onshore to the north of MB. Fluids are transparent with some coloration on the surrounding fine sediment. To the south of the port is the La Fossa area (LF). A cooler hydrothermal fluid point source was discovered near a mermaid statue in that area.

Concentrations of Hg were reported for La Fossa cone fumaroles (e.g., Bagnato, 2007; Ferrara et al., 2000; Zambardi et al., 2009) and groundwaters (Aiuppa et al., 2000; Bagnato et al., 2009). However, there were no data reported for Hg in the hydrothermal gases and fluids collected at the point of emission in Baia di Levante.

3. Methods

In June 2019 and September 2021, a total of 85 samples were collected across the bay and around the island for Hg_{diss} (filtered) and THg (unfiltered) in surface waters, the water column, and from hydrothermal point sources (PS), along with As, cations, and anions (Appendix 1 and 2). In a subset of samples, Hg was speciated (V25, V26, V29, V30, and V36), which included the determination of THg, Hg_{diss}, Hg^0, DMHg, and MMHg and required a sample volume of 1 L. Surface waters ($n = 32$) were collected by boat using 60 mL polypropylene syringes and filtered immediately onboard through a 0.45 μm membrane. Hydrothermal fluids were collected using pore fluid samplers constructed from PTFE tubing and 10 mL pipette tips at 10 cm sediment depth using polypropylene 60 mL syringes. Porewater temperatures were monitored at the pipette tip, and deviations in temperature were not observed during sampling. This ensured that samples were not contaminated with seawater. Measurements of pH (Halo Wireless pH meter, Hanna Instruments), conductivity and ORP (Myron Ultrameter) were immediately taken in the field. The subsample for anion analysis was filtered with a 0.45 μm syringe filter, and the subsamples for elemental analysis (ICP-OES and ICP-MS) were additionally preserved with 2% (m/v) concentrated nitric acid.

The syringes that were collected for Hg speciation were carefully expelled into a 1 L glass jar in the field lab for Hg^0 collection. To avoid the potential loss of Hg^0, utmost care was taken to prevent turbulent flow while transferring the sample.

A total of six gas samples were collected for analysis of Hg_{gas} (Table 1). Background surface seawater samples were collected in areas with no visible hydrothermal activity outside Baia di Levante to the east (V36) and on the other side of the island to the west (V47-V50).

Liquid Hg samples were collected as unfiltered and filtered (0.45 μm), stored and analyzed following the USEPA (2002) protocol with a Brooks Rand CV-AFS analyzer. The acidified samples arrived from the field in the laboratory and were held at 4 °C until analysis. On the day of analysis, 40 mL sample were transferred into a 60 mL Volatile Organic Analysis (VOA) glass vial with a PTFE lined cap. 400 μL acidified bromide/bromate (1:1 mixture of 0.01 M bromide/bromate solution (Tritrisol, Merck) and 32% hydrochloric acid (Optima grade, Fisher Scientific)) were added to the sample and left standing for at least 30 min at room temperature. The reactivity of the bromine chloride was then quenched by adding 100 μL 30% (m/v) hydroxylamine hydrochloride solution (ReagentPlus, 99%, Sigma-Aldrich). Elemental Hg was generated in the solution upon the addition of 200 μL 20% (m/v) tin(*II*) chloride solution (Reagent grade, Alfa Aesar). Each sample was analyzed in duplicate whenever the sample volume allowed. The limit of detection for this method in our laboratory was determined to be 0.04 ng/L ($n = 10$). The certified reference material ORMS-5 (elevated Hg in river water, National Research Council Canada) was used for quality control. The reference material is certified for a concentration of 26.2 ± 1.3 ng/L THg.

The sediment samples were digested in 10:3 aqua regia following Bloom et al. (2003) and THg was analyzed by CV-AFS. The certified reference material PACS-1, certified for a concentration of 4.57 ± 0.16 μg/g THg was used for quality control.

Hg^0 in the liquid phase was collected from selected samples (Table 2) by purging 1 L of hydrothermal fluid with Hg free nitrogen onto gold and carbo traps and analyzed by CV-AFS (Cossa et al., 2011; Lehnherr et al., 2011).

MeHg was analyzed by species-specific isotope dilution-gas chromatography-inductively coupled plasma-mass spectrometry (SSID-GC-ICP-MS) (Brombach et al., 2015). A 100 mL sample was spiked with a solution of $Me^{201}Hg$ (ISC Science, Spain) and left standing for an hour for equilibration. An optimal ratio of 4.25 for $Me^{201}Hg$ in the spike to $Me^{202}Hg$ in the sample was the aim of the spiking. Based on the assumption that 5% of THg was present as $Me^{201}Hg$, the amount of the enriched isotopic solution was calculated for the initial spiking. An addition of 5 mL of a 1 M acetic acid – acetate buffer at pH 3.9, prepared from trace metal grade acetic acid (Fisher Scientific) and 30 M NaOH (Suprapur, Merck), was added to the sample, and the pH was adjusted to 3.9 with sodium hydroxide (30 M, Suprapur, Merck). Subsequently, 1 mL propylation reagent (1 g sodium tetrapropylborate;Merseburger Spezialchemikalien, Germany) in 100 mL oxygen-free Milli-Q water was added to the sample followed by 200 μL n-hexane (Reagent Grade ACS, Riedel-de-Haen). The Hg species were extracted into the n-hexane phase by shaking for 10 min, and the n-hexane phase was analyzed using a Thermo Scientific Trace 1300 GC coupled to a Thermo Scientific Element 2 ICP-MS. A cyclonic spray chamber was attached to the transfer line just before the ICP torch for wet plasma conditions giving the option of plasma tuning and monitoring with an internal Thallium standard. General settings of the GC and the ICP-MS can be found elsewhere (Brombach et al., 2015).

Gas samples were collected into Tedlar© bags using a custom-built glass funnel connected to Teflon tubing in combination with a standard underwater lift bag. The lift bag was attached to lead weights which enabled the calculation of the gas volume collected, i.e., the volume of gas needed to displace enough seawater to lift the bag at a given depth and lead weight. In some instances, gas point sources were

Table 1
Concentrations of Hg in the gas phase on Vulcano.

Sample Number	Sample Description	Gas nmol/m^3
	Bambino	
V51	Low Tide	122
V52	High Tide	113
B-B-06	2021 Low Tide	120
B-MB	Mini-Bambino	282
	White Patch	
V29	White Patch 10 cm	7
V39	White Patch T Map: White	5
	Baia di Levante	
V30	Subaerial low-Cl	3
V42	Shore Sample	1768
V43	Rock Boulder at Mud Bath	1817

Table 2
Concentrations of dissolved Hg^0 in collected fluid samples from Vulcano.

Sample Number	Sample Description	Hg^0
		pM
V36	Background (Vulcano)	0.98
B-B-06	Bambino	7.27
V29	White Patch 10 cm	5.33
V30	Subaerial low-Cl	1.52
V25	Tidal Cave	3.3
V26	Submarine Cave	2.58

located at depths too shallow to use the lead weights. In these instances, gas sample bags were filled as much as possible without damaging the sample bag. H_2S was removed from the gas in an alkaline trap, to prevent the formation of HgS within sample vials. The sample was then trapped in 0.5 M permanganate solution in 2 N sulfuric acid and analyzed by CV-AFS as THg (Brombach and Pichler, 2019).

Anions were analyzed using a Metrohm 883 Basic IC plus instrument fitted with a 5 µL injection loop and a Metrosep A Supp5 (150 × 4.0 mm; 5 µm) column for anion separation in combination with a mobile phase consisting of 3.2 mmol/L Na_2CO_3 (Analytical reagent grade, Fisher Scientific) and 1.0 mmol/L $NaHCO_3$ (puriss. p.a., ≥ 99.7%, Sigma-Aldrich). Quality control was assured with an internal laboratory standard and the artificial seawater standard IAPSO. Major cations were measured by inductively coupled plasma-optical emission spectrometry (ICP-OES) using a Perkin Elmer Optima 7300 DV instrument. Quality control was assured by using the EnviroMAT Groundwater Low (ES-L-2) and High (ES-H-2) standards and a certified seawater (CRM-SW, High Purity Standard). Trace elements were analyzed by inductively coupled plasma-mass spectrometry (ICP-MS, Element 2 Thermo Scientific). Quality control was identical to that of the ICP-OES measurements.

The flux (pmol/m^2/h) of Hg^0 to the atmosphere from each of the sampling sites was calculated using the equations by Liss and Slater (1974) (1) and Wanninkhof (1992) (2), as implemented by Wängberg et al. (2001), where DGM is the dissolved gaseous Hg concentration, TGM is an approximate gaseous Hg concentration for the area of Sicily as field blank values were below detection limits (10.86 pmol/m^3 (Kotnik et al., 2014)), k_w (cm/h) is the gas transfer velocity, u_{10} is the wind speed at 10 m height, Sc_{Hg} is the Schmidt number for Hg in seawater and Sc_{CO2} is the Schmidt number for CO_2 in seawater (Kuss et al., 2009), and H′ is the dimensionless Henry's law constant as calculated by Clever et al. (1985) (3). An approximate value was used for atmospheric Hg (7.5 pmol/m^3), and the percent volatile Hg^0 was assumed to be 10% of Hg_{diss} in seawater samples (Horvat et al., 2003). Schmidt numbers 689 for Hg and 660 for CO_2 were used.

$$Flux\ to\ the\ Atmosphere = k_w\left(DGM - TGM/_{H'}\right) \quad (1)$$

$$k_w = 0.31u_{10}^2\left(Sc_{Hg}/_{Sc_{CO2}}\right)^{-0.5} \quad (2)$$

$$H' = exp\left(\frac{-4633.3}{T_w} + 14.53\right) \quad (3)$$

4. Results

4.1. Seawater

In general, the surface water samples of Baia di Levante, outside of the mud bath area (MB), had similar concentrations of cations, anions, and metals as background seawater (Appendix 1). Significant deviations were observed in samples from areas with visible hydrothermal influences. These variations included a lower pH and elevated concentrations of SO_4, Si, H_2S, Sr, Mn, THg, and Hg_{diss} (Figs. 3 and 4). Among the surface water samples outside MB, a positive linear trend was observed between THg and Hg_{diss} (Fig. 5). The samples within the Vulcano Port area (V04 to V06, V10 to V12, and V16 to V17) were not included within the surface maps to improve data visualization.

In MB, high THg concentrations were observed in seawater and gas samples (Fig. 4). Samples taken at the orifices of two-point sources (Rock Boulder (V43) and Shore Sample (V42)) near the beach contained up to 2800 pM THg and 270 pM Hg_{diss} in 2019 (Appendix 3) with over 1800 nmol/m^3 Hg^0 in the emitted gas phase. Surface water samples above the point sources (V17 and V18, respectively) were higher than the surrounding surface water samples (Appendix 1). Hg_{diss} concentrations were lower closer to shore near the rocky outcropping and higher in areas of gaseous point source activity.

To the east of MB, white mats were observed. There, concentrations of THg in the gases were low (5 to 7 nmol/m^3) (Table 3), while pore fluids were low to high in THg (7 to 276 pM) and Hg_{diss} (0 to 7 pM) (Appendix 1). A significantly lower pH (pH 6.7) than that of seawater (pH 8.1) was observed above the white mats at location V15. Three vertical water column samples were collected at that station. The concentration of THg decreased substantially from 71 pM at the surface (V34) to 5 pM at a depth of 3 m (V33) and 3 pM at a depth of 5 m (V32).

Flux to the atmosphere was estimated at each surface site and ranged from 0.1 to 19.6 pmol/m^2/h^1 in 2019 (Appendix 2). Estimations for the MB area ranged between 1.4 and 9.0 pmol/m^2/h^1. Emission rates were highly dependent on Hg_{diss} concentrations. This is not necessarily surprising, as other factors affecting emission rates (wind speed,

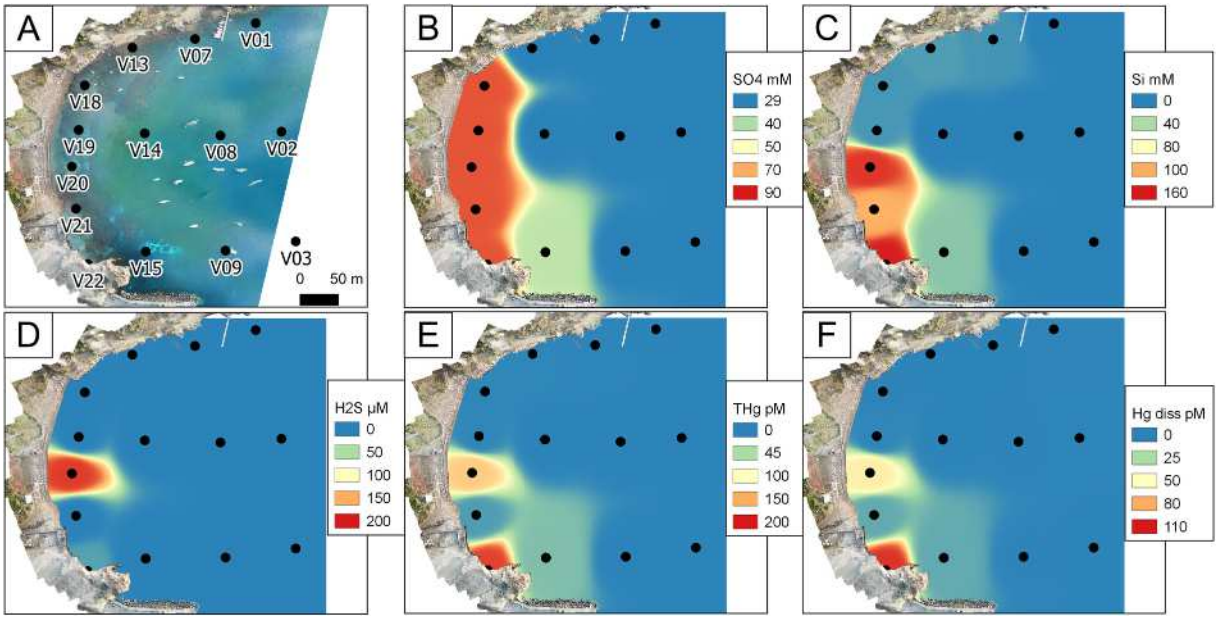

Fig. 3. Surface water maps of 2019 data of A) sample locations, B) SO4 (mM), C) Si (mM), D) H2S (µM), E)THg (pM), and F) Hgdiss (pM). Maps were generated in QGIS. For mapping purposes, values below detection limits were replaced with 0. Distance coefficient (P) was 6.5. Output raster size was 1026 by 2019.

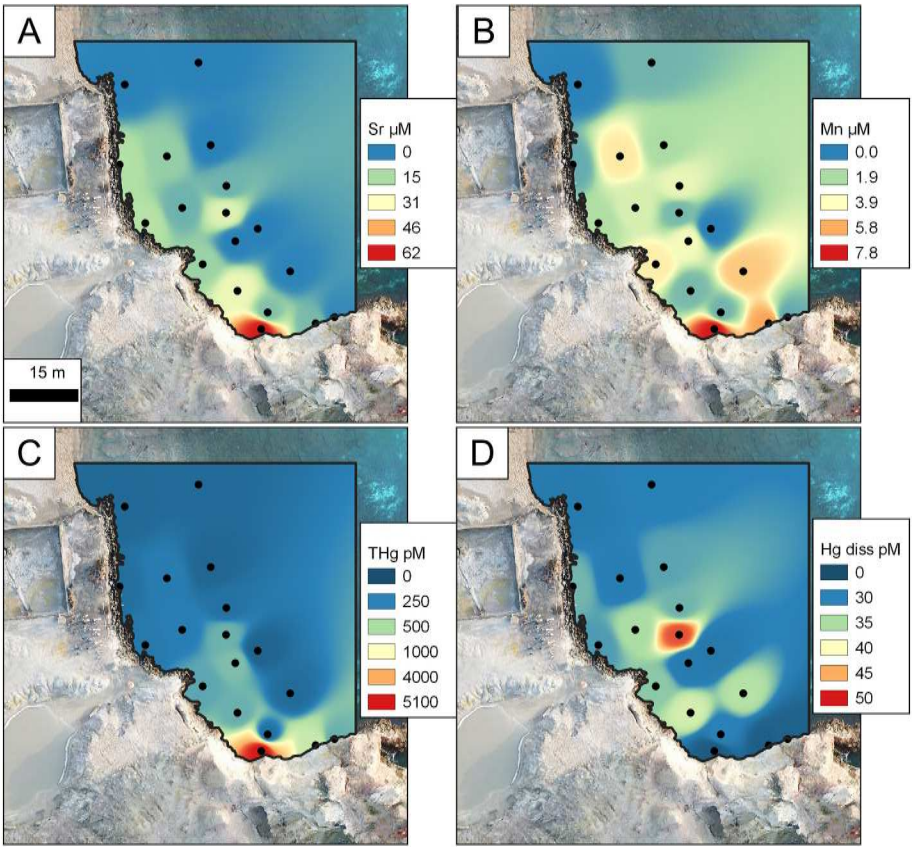

Fig. 4. Surface seawater water concentrations for September 2021 within the MB area of A) Sr (µM), B) Mn (µM), C) THg (pM) with extreme concentration gradient (3 m) highlighted by white points, and D) Hgdiss (pM). Maps were generated in QGIS. For mapping purposes, values below detection limits were replaced with 0. Distance coefficient (P) was 5. Output raster size was 1000 by 986.

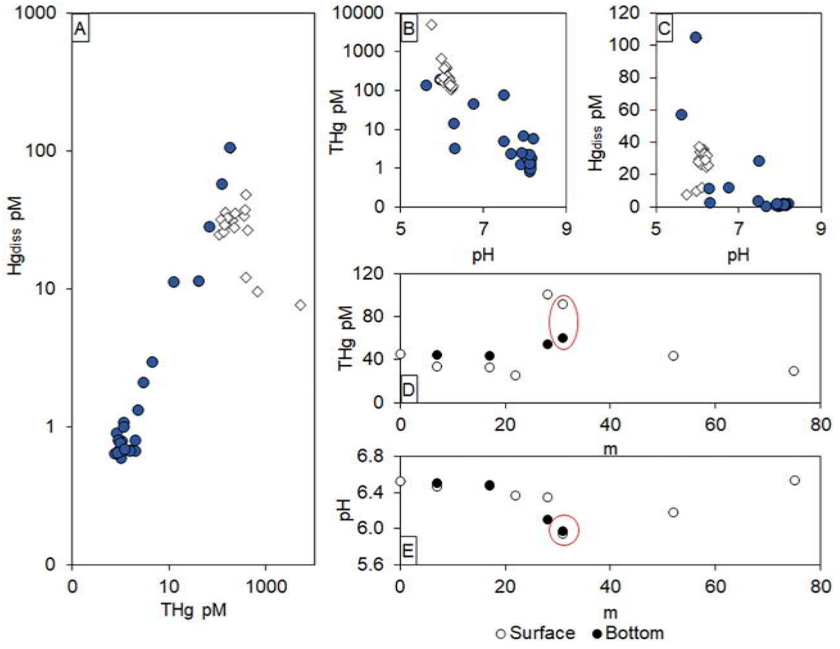

Fig. 5. Seawater (blue circles) and MB (white diamonds) concentrations of A) THg (pM) vs Hgdiss (pM), B) THg (pM) vs pH, C) Hgdiss (pM) vs pH. Bambino transect with distance (m) from shore. D)THg (pM) and E) pH. The location of Bambino is circled in red. (For interpretation of the references to colour in this figure legend, the reader is referred to the web version of this article.)

Table 3
Concentrations of Hg in the gas phase.

Sample Number	Sample Description	THg Gas
		nmol/m^3
	Bambino	
V51	Low Tide	122
V52	High Tide	113
B-B-06	Bambino Transect	119.89
B-MB	Mini-Bambino	281.65
	White Patch	
V29	White Patch 10 cm	7
V39	White Patch T Map: White	5
	Subaerial and Tidal Sites	
	Baia di Levante	
V30	Subaerial low-Cl	3
V42	Shore Sample	1768
V43	Rock Boulder at Mud Bath	1817

atmospheric Hg concentration, etc.) were considered the same for all sites.

The Bambino gaseous point source contained 113 nmol/m^3 Hg at high tide and 122 nmol/m^3 at low tide in 2019 and 120 nmol/m^3 in 2021 (Table 3). It should be noted that the Bambino site was too shallow to use lead weights to determine the gas collection volume. Due to the potential for sampling error, those two values were considered the same for both low and high tide and 2019 and 2021. An emission rate was measured at the Bambino site. A 2 L graduated cylinder was filled with seawater and placed over the point source. The rising gas displaced the seawater from the cylinder, with the timing of full displacement indicative of an emission rate. However, gas emissions exceeded 2 L/s when approximations were attempted. The cylinder overflowed with gas immediately. Therefore, a minimum of 2 L/s was established for calculation purposes. Under these assumptions, Bambino contributed 235 pmol/s of Hg to the area on average. In surface waters directly above Bambino (V20), 131 pM THg was observed in 2019, with 56 pM as Hg_{diss} (Appendix 1). A sample of Hg^0 from surface waters was taken above Bambino in 2021 with a concentration of 7.3 pM (Table 2), with THg 92 pM (Appendix 1). The resulting flux to the atmosphere using the Hg^0 concentration was estimated at 13.6 pmol/m^2/h^1.

A surface and bottom water transect, including Bambino (B-S-06 and B-B-06), were completed at ebb tide (Appendix 1, Fig. 5). Additional samples were taken on separate days (B-01 and B-02). Surface water samples only were collected at stations where the depth was too shallow (B-S-01 and B-S-04) or too deep to sample without diving equipment (B-01 and B-02). Concentrations of THg ranged from 33 and 101 pM at the surface and 43 to 61 pM at depth. The concentrations of THg were highest directly above or adjacent to Bambino in the surface waters. Bottom water concentrations were similar to surface water concentrations at stations B-S-02 and B-S-03 but were significantly less than surface waters at B-S-05 and B-S-06. Temperatures were the same for all samples except for B-01 and B-02. Values of pH decreased with proximity to Bambino.

4.2. Pore fluids

In general, pore fluid samples had a lower pH, higher temperature, elevated concentrations of Ca, K, Li, Mn, Si, H_2S, THg, and Hg_{diss}, and lower concentrations of Cl, Br, Na, and Sr than the background sample (Appendix 3). No linear relationship was observed between THg and Hg_{diss}. The tidal cave (V25 and F-01) was depleted in Cl, Br, Mg, Na, and Sr but contained elevated concentrations of THg, Si, Fe, and SO_4. The two additional point sources on the rocky outcropping on the port side (F-02 and F-03) were similar in anion and cation concentration to the tidal cave, but with higher As (0.5 and 1.3 μM), lower THg (27 and 26 pM) and Hg_{diss} (6.5 and 5.5 pM) concentrations. The shore sample contained depleted but near background concentrations of major constituents. However, concentrations of THg, Hg_{diss}, Si, and Li were elevated. An onshore subaerial site (V30) was sampled during an ebb tide. The chemical composition of V30 was depleted in major constituents, acidic, and elevated in Si and THg. Gas concentrations of Hg were low (3 nmol/m^3).

The LF samples contained hot, acidic fluid with close to background concentrations of major constituents. THg and Hg_{diss} were elevated in all samples but highest in the sample with no Fe or H_2S. The fluid of V27 was similar to the La Fossa Submarine Cave sample (V26), except for higher As concentrations (3.3 μM). Si concentrations were high in all samples. A similar chemical composition was observed for a nearby submarine point source (V26).

A five-point transect was completed in 2019 of porewaters within the white mat area. Each sample represented different environmental conditions: seagrass (V37), sand (V38), a dense white mat (V39), bubbling sand (V40), and a sparse white mat (V41). Each sampled location showed differences in chemical composition (Appendix 3). Metals and metalloids (Fe, Mn, Si, Hg, As) and H_2S were elevated relative to seawater in bubbling and white mat samples. However, Mg was not depleted. The sample named 'seagrass' was near white mat activity; however, the chemical composition was similar to seawater except for elevated THg and Si.

4.3. Sediments

Sediments were collected as general representations of background (Black Beach, 0.03 nmol/g), the MB area (MB-15, 2.4 nmol/g), and an active point source (B-Bowl, 49.5).

4.4. Gases

Gases were collected from point sources onshore, nearshore, and the white mat area (Table 1). Concentrations ranged from 3 nmol/m^3 onshore, 113 to 1817 nmol/m^3 in nearshore samples, and 5 to 7 nmol/m^3 in white mat samples.

4.5. Speciation

Neither MMHg nor DMHg was detected in the fluids from point sources of the Vulcano MSWHS. Measurements of volatile Hg ranged in concentration from 0.98 to 7.27 pM. Hg^0 pM.

4.6. Chloride ratios

Ratios of conservative elements (e.g., Cl, Na, Mg, Ca, K) follow linear trends in seawater, with changes in concentration due primarily to mixing with fresh water. Hydrothermal and seawater samples were distinctly different with respect to conservative elements (Fig. 6). The seawater and MB samples generally followed a linear trend between Na and K when normalized to Cl, while hydrothermal pore fluid samples did not (Fig. 6B). High THg concentrations in hydrothermally influenced samples were associated with lower Mg/Cl and K/Cl (g) ratios (Fig. 6B and C).

5. Discussion

5.1. Overview

The enrichment of Hg in surface water samples in Baia di Levante was due to intense and shallow hydrothermal activity (Fig. 7). Fluxes of fluids and gases containing high concentrations of Hg relative to background concentrations mix with overlying seawater upon emission. However, due to the buoyancy of the warm fluid, significant concentrations of Hg accumulated in the surface waters. Removal of Hg from

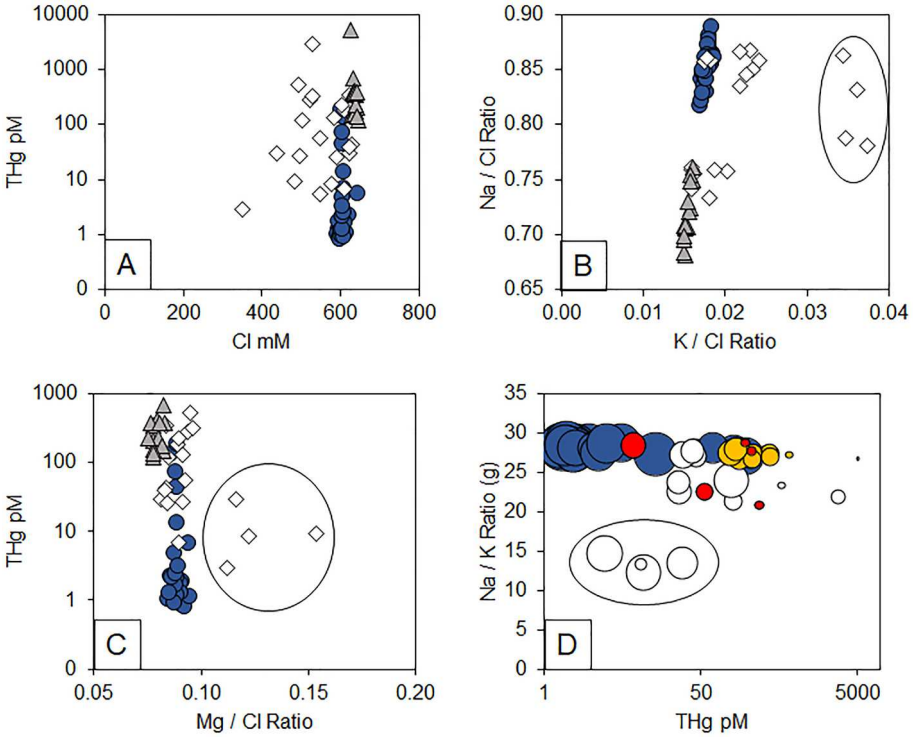

Fig. 6. Plots of hydrothermal (white diamonds), MB seawater (grey triangles), and seawater (blue circles) samples. LF samples are circled. A) THg (pM) vs Cl (mM), B) Na/Cl vs K/Cl ratio, C) THg (pM) vs Mg/Cl ratio, D) Na/K ratio (mg) vs THg (pM) in seawater (blue), hydrothermal (white), white mat area (red), and MB (yellow), with bubble size indicating percent THg as Hgdiss. MB samples contained greater THg concentrations compared to seawater throughout Baia di Levante but maintained Na and K linear mixing trends. Hydrothermal samples did not show linear mixing trends. (For interpretation of the references to colour in this figure legend, the reader is referred to the web version of this article.)

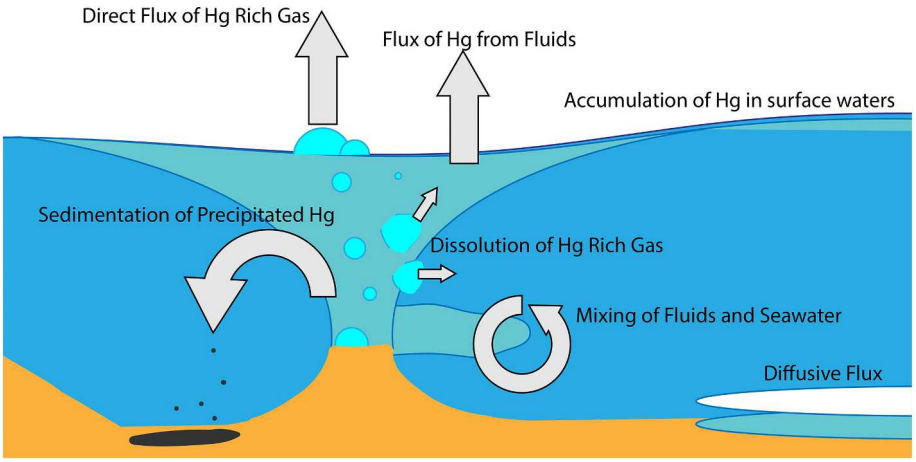

Fig. 7. Schematic of Hg cycling from Vulcano point sources. Fluxes of fluids mix with the surrounding seawater, however due to the buoyancy of the warm fluid, significant concentrations of Hg accumulate in the surface waters. Due to changes in temperature and redox conditions, Hg may also precipitate from the water column. Gaseous Hg species may partially or fully dissolve in the water column during their ascent to the surface. In cases of shallow depth and high rates of gas emission, gaseous Hg may primarily be emitted to the atmosphere. For the Vulcano system, diffusive fluxes did not appear to play a large role in Hg accumulation within surface waters.

Baia di Levante included flux to the atmosphere from fluids, sedimentation due to changing redox conditions and temperature (see 4.2), and dilution and transport in the water column.

5.2. Hg in Bahia di Levante seawater

The dominant source of THg to the surface water in Baia di Levante was the accumulation of buoyant hydrothermal fluid. This was demonstrated by water column samples collected at V15, the Bambino transect (Fig. 5), and was previously established for other systems and metals (Pichler et al., 2019; Pichler et al., 1999b; Roberts et al., 2021). Alternative sources of Hg to Baia di Levante (anthropogenic influences and atmospheric deposition) were not significant compared to the MSWHS discharge. Increases in THg concentrations in proximity to the coast, and therefore human activity, were observed (Fig. 3). However, these enrichments were associated with hydrothermal activity. In areas with increased boating activity and fewer hydrothermal influences, THg values were equivalent to or below background values. Atmospheric deposition is known to generate supersaturated concentrations of Hg in the ocean surface and mixed layer waters due to Hg^0 oxidation (Fitzgerald et al., 2007). However, the magnitude of supersaturation due to atmospheric deposition was found to be comparatively low in the Mediterranean (e.g., Cossa et al., 1997a; Horvat et al., 2003). In addition to physical proximity to hydrothermal sources, elevated Hg concentrations were observed together with elevated concentrations of As, deviation from linear mixing patterns of cations and anions (Fig. 6), and a lower pH than background seawater. These factors are commonly associated with hydrothermal activity (e.g., Khimasia et al., 2021; Pichler et al., 1999b; Pichler et al., 1999c; Price et al., 2013a; Roberts et al., 2021). The mobilization of As by hydrothermal systems due to changing redox conditions is well established (Pichler et al., 1999b; Price and Pichler, 2005) and both As and Hg belong to the "epithermal

suite" of elements (Au, Ag, Te, Se, Hg, As, Sb, and Tl) (Berger and Eimon, 1983; Saunders and Brueseke, 2012; Saunders et al., 2008). The grouping is generally controlled in their similar behavior by two main properties: (1) they are all soft Lewis acids and therefore form covalent bonds with soft Lewis bases, and (2) they have similar volatility resulting in their liberation from the mantle. Several studies identified enrichments of epithermal suite elements in MSWHS (Gamo and Glasby, 2003; Johnson and Cronan, 2001; McCarthy et al., 2005; Prol-Ledesma et al., 2004; Roberts et al., 2021) and following mixing with seawater, hydrothermally derived As and Hg have been shown to accumulate in surface waters (Pichler et al., 2019; Pichler et al., 1999b; Roberts et al., 2021). Therefore, elevated concentrations of THg and Hg_{diss} were considered to be caused by the hydrothermal activity in Baia di Levante.

The fate of Hg from the MSWHS of Baia di Levante is strongly tied to surface water conditions because, due to hydrothermal fluid buoyancy, Hg accumulates at the surface and is potentially transported over large distances. For example, Leal-Acosta et al. (2013) reported dissolved Hg at a significant distance (km) away from hydrothermal sources in the Gulf of California. Elevated Hg_{diss} concentrations in Baia di Levante, which trended positively with THg in surface waters outside of MB (Fig. 5), indicated the potential for transport and biological uptake. However, the surface water concentrations of Hg in Baia di Levante did not mirror the extent of other hydrothermal indicators (e.g., SO_4 and Si, see Fig. 4). Despite high concentrations of THg and Hg_{diss} in surface waters directly above or adjacent to point sources (e.g., MB-01), surface waters decreased in THg from 5110 pM to 164 pM over a distance of <5 m (Fig. 4). In contrast, Hg_{diss} increased from 7.6 pM to 29.8 pM. Additionally, a negative trend was observed between pH and THg and Hg_{diss} (Fig. 5). With an increasing seawater pH, the adsorption of Hg onto particles is enhanced, specifically for clay minerals and iron oxyhydroxides (Anderson, 1979). The sedimentation of particles, as previously discussed for other submarine and subaerial systems (e.g., King et al., 2006; Leal-Acosta et al., 2010; Roberts et al., 2021), would result in a reduction of THg in addition to Hg_{diss} due to sedimentation. Sediment collected in the MB (2.42 nmol/g) and Bambino (49.52 nmol/g) areas reflected this process when compared to sediment collected within Black Beach (0.03 nmol/g). A previous study of a subaerial system showed a similar pattern, where THg concentrations rapidly declined away from hydrothermal sources, with amorphous S precipitates dominating removal (King et al., 2006). In accordance with those findings, surface waters above the MSWHS in Bahia di Levante could be considered a reservoir of THg and, therefore, may play a crucial role in the ultimate fate of Hg discharged from any MSWHS.

The MSWHS in Baia di Levante discharged large volumes of hydrothermal gases, which rapidly percolated through the water column and into the atmosphere. Therefore, gas emissions from this system directly affected the overlying water through bubble dissolution and the atmosphere through evasional and ebullitive flux (Fig. 7). Previous studies indicated efficient dissolution of gases in deep and shallow waters (e.g., McGinnis et al., 2011; Zhao et al., 2016), and Pichler et al. (1999a) highlighted the impact of gases on water chemistry and sedimentation. The highest calculated atmospheric flux of Hg to the atmosphere from surface waters (19.6 pmol/m^2/hr) was significantly higher than that observed by Roberts et al. (2021) for the Milos MSWHS (2.7 pmol/m^2/hr) but not as high as the flux calculated by Bagnato et al. (2017) for the Panarea MSWHS (45 pmol/m^2/hr). While not intended to provide precise evasional flux measurements, the calculation illustrated the magnitude of hydrothermal impacts on surface waters with distance from point sources. Significant differences were observed in the surface waters of Baia di Levante. The highest were near, or directly above, shallow point sources. The Hg in hydrothermal gases is presumed to be Hg^0 (Brombach and Pichler, 2019). Bambino represents an ideal point source to study, with a high volume of gas output at a shallow depth where evasional and ebullitive flux are potentially significant. However, only 43% of the THg was Hg_{diss} above Bambino, and <10% of Hg_{diss} was Hg^0. After a distance of 9 m to the west and 21 m to the east of Bambino, the THg concentrations in surface water were reduced to 28% and 48% of the Bambino surface water concentration. This result was surprising, given the numerous point sources at a lower depth east of Bambino (Fig. 2F). The formation of bound Hg species was likely due to oxidative reactions, which rapidly reduced Hg_{diss} away from point sources. The rapid (first-order rate constant $k = 0.1\ h^{-1}$) oxidation of Hg^0 before reaching surface waters is expected to be driven by photochemical reactions and enhanced with the presence of Cl (Amyot et al., 1997; Lalonde et al., 2001). The oxidation of Hg^0 to Hg^{2+} prevented the evasion of dissolved Hg^0 to the atmosphere and, thus, preserved Hg in seawater.

It should be noted that sample B-S-05, located 3 m west of Bambino, was higher in THg concentration than B-S-06 taken directly above Bambino in the bubbling area. Two scenarios could account for this phenomenon. First, transport away from Bambino during ebb tide would result in overall eastward movement of surface waters, although the distance between the stations was minimal. Displacement and mixing due to Bambino itself or anthropogenic activities (e.g., boating activities) could account for an increase in concentrations adjacent to the point source. This scenario is less likely, as the pH is lowest at the Bambino site, with a significant difference between the surface and bottom waters pH at B-S-05. This is despite the higher THg concentrations in the surface water samples than in the bottom water samples. Second, the slight decrease in concentration at B-S-06 could be due to intense bubbling directly above the point source. The decrease was approximately equal to the concentration of Hg^0 at B-S-06, which was taken <1 m away from the bubbling area. While oxidation of Hg^0 is expected to be efficient at this location, Hg^0 present in surface seawater would be expected to be transferred to the atmosphere due to wind and bubbling.

5.3. Source of Hg

The MSWHS on Vulcano is thought to be fed by a combination of meteoric water, seawater, magmatic water, and a boiling aquifer beneath the bay (Aiuppa et al., 2020; Federico et al., 2010; Fulignati et al., 1998; Inguaggiato et al., 2012; Madonia et al., 2015; Oliveri et al., 2019). The boiling aquifer resulted in a Hg-rich vapor phase that was the primary contributor of Hg to the system. Hg concentrations in groundwaters and subaerial fumarole gases on Vulcano are linked to magmatic and hydrothermal origins (Aiuppa et al., 2007; Bagnato et al., 2009; Nuccio et al., 1999; Paonita et al., 2002; Zambardi et al., 2009). Bagnato et al. (2009) concluded that the THg found in Vulcano groundwaters was of hydrothermal origin and transported as Hg^0 in a vapor phase and oxidized to Hg^{2+} in shallow groundwaters. A similar scenario, i.e., a Hg-rich vapor as the source for Hg in the Bahia di Levante MSWHS should also be likely. Low-Cl, high THg hydrothermal fluids are discharging in Baia di Levante (Fig. 6A), which would indicate the condensation of a hydrothermal vapor low in Cl, but enriched in Hg. The white patch area, where diffuse fluid flow and limited gas emission are present, also revealed higher THg concentrations in pore fluids at or below background Cl concentrations.

In a previous study, Roberts et al. (2021) described the MSWHS on the island of Milos with regard to Hg concentrations. There, elevated THg was associated with high Cl and low Na/K ratios, which indicated a greater arc-magmatic input coupled with fast ascension rates. This result was surprising, given the volatility of Hg and its association with the hydrothermal vapor phase in the subsurface (Barnes and Seward, 1997; Varekamp and Buseck, 1984). In contrast to the Milos system, the Hg concentrations of the MSWHS of Baia di Levante were associated with low-Cl fluids, a more intuitive result given the above. The presence of Hg, and its association with major elements, is descriptive of significant subsurface properties and processes. The proposed subsurface reactions can be supported by the relative concentrations and behavior of Hg in comparison to major elements. This study supports previous work associating localized elevated environmental Hg concentrations in the

areas surrounding hydrothermal systems (Leal-Acosta et al., 2018; Leal-Acosta et al., 2010; Prol-Ledesma et al., 2004; Roberts et al., 2021). In particular, this study and Roberts et al. (2021) emphasize the importance of sampling both fluids and gases from MSWHS. In two distinct sampling areas with notably different subsurface processes, the concentrations of THg, Hg_{diss}, and Hg_{gas} demonstrate reactions in the shallow subsurface. These reactions played a crucial role in Hg emissions from MSWHS and potential further transport.

Volatile species constituted a considerable portion of Hg_{diss} in some samples (Table 2). This finding further supports hydrothermal vapor as the primary Hg source in this system. The Hg^0 concentrations increased linearly with increasing temperature (Fig. 8). Similarly, pH decreased with increasing temperature. While not definitive, temperature and increasing acidity indicate hydrothermal activity (e.g., Khimasia et al., 2021; Roberts et al., 2021). Longer, slower transport increases the potential for redox reactions and therefore changes in speciation, particularly for the white mat and sedimented areas (Hsu-Kim et al., 2013; Roberts et al., 2021). The hotter, more acidic fluid may indicate a more direct, less seawater diluted hydrothermal gas and fluid flow. Higher Hg^0 concentrations would reflect greater proportions, or faster ascension of, the hydrothermal vapor phase. In one instance (V26), the volatile measurement exceeded Hg_{diss} concentrations. This result may be from measurement error or the result of volatile species bound to particulates (Wang et al., 2015).

5.4. White mat area

The hydrothermal white mat areas did not contribute significantly to THg concentrations in Baia di Levante. While the pore fluids concentrations of THg were generally high (Appendix 3), the evidence did not support significant diffusive transport to the overlying water column. White mat areas have previously been found to affect Hg concentrations in the gas streams of MSWHS through subsurface removal of Hg species (Roberts et al., 2021). The white mat area of Baia di Levante was the only sedimented area where gases were measured (V29, V39). Gas flow was low, and Hg concentrations were between 5 and 7 nmol m^{-3} (8). Nearby (V15) water column measurements at depths of 2.7 m and 5.4 m did not indicate vertical transport as a significant contributor to surface concentrations. Additionally, the Na/K ratios of the white mat area fluid samples indicated slower ascension rates through the subsurface (Fig. 6D) (Khimasia et al., 2021; Nicholson, 1993; Roberts et al., 2021). Slower ascension rates were previously hypothesized to reduce THg concentrations in gases and fluids through HgS formation in the subsurface (Roberts et al., 2021). Contributions of the white mat area were therefore not significant to surface concentrations due to limited surface area in Baia di Levante and lack of vertical transport.

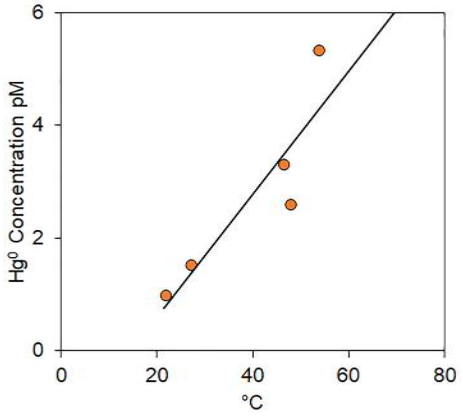

Fig. 8. Plot of Hg0 (pM) and temperature (°C).

5.5. Bambino

The point sources responsible for elevated Hg concentrations in Baia di Levante surface seawater were not necessarily those with the highest Hg concentrations. The intensity and volume of flow were also important factors. The Bambino point source had less Hg in the gas phase (113 to 121 nmol/m^3) than the MB point sources (1800 pM) but at the same time had a higher emission rate. A nearby smaller point source (Mini-Bambino) emitted gases with a higher Hg concentration (281 nmol/m^3), however, it emitted significantly less gas volume than Bambino. Further east of Bambino, several small point sources emitted gases at 2 m depth (Fig. 2F). Despite the larger overall number of point sources east of Bambino, the surface water concentrations of THg were highest near Bambino. The THg concentrations observed in the 2021 transect decreased from 92 pM to 26 pM over a distance of 9 m towards the shoreline and to 44 pM over a distance of 21 m to the east. Despite many point sources with elevated THg concentrations (342 pM THg, VB-7B), surface water concentrations were not higher than concentrations observed closer to shore. Additional water depth led to two significant differences. First, water depth increases the dilution of hydrothermal fluids and gases by increasing the water volume between sources and the surface. Second, there is additional potential for the removal by precipitation and sedimentation, since fluid and gas are exposed to oxygenated seawater and photochemical reactions for a longer period before reaching the surface (Davey and van Moort, 1986; Lalonde et al., 2001). Therefore, despite lower concentrations of Hg_{gas} than MB point sources, the Bambino area significantly impacted surface water concentrations of THg and Hg_{diss} (56 pM), as well as pH (Fig. 5).

Bambino was estimated to output 235 pmol/sec Hg, with a surface water atmospheric flux of 25 pmol/m^2/h. As a primarily gaseous point source (e.g., Fig. 2E), a surprisingly significant portion of THg was bound to particulates in the fluid sample in 2019 (75 pM). Despite high Hg_{diss} concentrations in 2019 (56 pM), Hg^0 was only 7.3 pM when measured in 2021. Amyot et al. (1997) estimated Hg^0 loss due to oxidation as roughly half of the flux to the atmosphere at a depth of 1 m. This rate of oxidation would account for the high Hg concentration bound to particulates despite a source enriched in Hg^0. The emission of THg from Bambino is 10-times the rate of flux from the seawater surface to the atmosphere. This leaves a significant portion of THg not accounted for. If all THg from Bambino remained within the water column, concentrations of THg in B-S-06 would exceed 1 nM in five minutes despite the flux of Hg_{diss} from the surface to the atmosphere. Considering THg concentrations throughout Baia di Levante and the Bambino area (Figs. 3 and 4), transport away from the site was limited.

Additionally, THg from Bambino affected surface seawater but had little impact on the bottom water concentrations (Fig. 5). Therefore, THg emitted by Bambino not accounted for in the surface was likely emitted directly to the atmosphere. The study of oxidation rates at the concentrations and environmental conditions at hydrothermal systems is necessary to support this hypothesis further.

5.6. La Fossa (LF) samples

The LF samples (V26, V44-V46) likely originated as condensed vapors from the La Fossa crater, which were transported downslope. This contrasts the Baia di Levante samples, which were likely generated by a boiling hydrothermal aquifer. La Fossa crater gases are a mixture of magmatic water and seawater (Chiodini et al., 1995), and soil temperatures exceed 100 °C with concentrations averaging 12 nmol/m^3 Hg_{gas} (Aiuppa et al., 2007; Barde-Cabusson et al., 2009; Zambardi et al., 2009). Magmatic vapors condense to form a salt-rich, acidic fluid, which is then transported and diluted by seawater or groundwater (Madonia et al., 2015; Williams-Jones and Heinrich, 2005). Oxidation of Hg caused by low pH drives speciation to Hg^{2+} and changes in temperature and oxidation remove Hg from solution, particularly at near-surface pressures and temperatures (Varekamp and Buseck, 1984; Williams-

Jones and Heinrich, 2005). We propose that the LF samples resulted from mixing between condensed La Fossa crater vapor, meteoric water, and seawater. Notably, the LF samples were below 65 °C. This temperature was previously associated with a turning point of lower THg concentrations on the island of Milos (Roberts et al., 2021). Bagnato et al. (2009) discussed the groundwaters of Vulcano, where increases in THg were associated with SO_4 and therefore hydrothermal or magmatic activity. However, the LF samples contain higher cation/anion concentrations and significantly lower THg concentrations than can be explained by mixing between seawater and groundwater. Similarly, the influence of a hydrothermal brine is unlikely. The LF samples do contain high Mn concentrations in comparison to background samples. High Mn is associated with rising hydrothermal brines (Valsami-Jones et al., 2005). Models of the Vulcano system also indicate the existence of a rising hydrothermal brine (Bolognesi and D'Amore, 1993) with the potential to affect groundwaters (Bagnato et al., 2009) and subaerial fumaroles (Chiodini et al., 1995; Di Liberto et al., 2002). However, low Cl coupled with high Li concentrations in these samples does not support this theory.

6. Conclusions

The Vulcano system highlights the complexity of Hg cycling in MSWHS. The Vulcano system demonstrated the direct influence of gaseous point sources on the Hg concentration in surface waters followed by rapid oxidation. Hg concentrations (THg and Hg_{diss}) were elevated in Baia di Levante, particularly in the MB area, due to hydrothermal activity as highlighted by water column concentrations, hydrothermal fluid and gas THg concentrations and surface water maps of THg. The area north of Vulcano port and close to shore contained the highest Hg concentrations in fluids and gases. Condensed vapor from La Fossa crater and diffuse venting from white mat areas are unlikely to contribute significantly to surface coastal Hg concentrations for this system. Therefore, the elevated THg in Baia di Levante was due to hydrothermal point sources located in the shallow waters of the bay.

The Hg present in the hydrothermal system of Vulcano impacts local groundwaters and the coastal waters of Baia di Levante and constitutes a natural source of Hg to the atmosphere. High volumes of gas emissions rich in Hg, coupled with highly elevated localized concentrations of THg and Hg_{diss}, warrant further investigation, particularly into the sediments and organisms of Baia di Levante.

Declaration of Competing Interest

The authors declare that they have no known competing financial interests or personal relationships that could have influenced the work reported in this paper.

Acknowledgments

The authors would like to thank Dr. Cornelius Brombach, Dr. Daniel Doischer and Amina Walkiewicz who assisted in the field, and to Henning Fröllje for laboratory support. This work was supported by the Deutsche Forschungsgemeinschaft (DFG) grant PI 746/10-1 to TP.

Appendix A. Supplementary data

Supplementary data to this article can be found online at https://doi.org/10.1016/j.marchem.2022.104147.

References

Aiuppa, A., Dongarrà, G., Capasso, G., Allard, P., 2000. Trace elements in the thermal groundwaters of Vulcano Island (Sicily). J. Volcanol. Geotherm. Res. 98 (1), 189–207.
Aiuppa, A., et al., 2007. Real-time simultaneous detection of volcanic hg and SO2 at la fossa crater, vulcano (aeolian islands, sicily). Geophys. Res. Lett. 34 (21).
Aiuppa, A., et al., 2020. Volcanic CO2 seep geochemistry and use in understanding ocean acidification. Biogeochemistry. 152 (1), 93–115.
Amyot, M., Gill, G.A., Morel, F.M., 1997. Production and loss of dissolved gaseous mercury in coastal seawater. Environ. Sci. Technol. 31 (12), 3606–3611.
Anderson, A., 1979. Mercury in soils. In: Nriagu, J. (Ed.), The Biogeochemistry of Mercury in the Environment. Elselvier, Amsterdam, pp. 79–112.
Aubert, M., Diliberto, S., Finizola, A., Chébli, Y., 2008. Double origin of hydrothermal convective flux variations in the Fossa of Vulcano (Italy). Bull. Volcanol. 70 (6), 743–751.
Bagnato, E., 2007. Estimates of Mercury Emission Rates in Active Volcanic Systems.
Bagnato, E., et al., 2009. Mercury concentration, speciation and budget in volcanic aquifers: Italy and Guadeloupe (Lesser Antilles). J. Volcanol. Geotherm. Res. 179 (1–2), 96–106.
Bagnato, E., et al., 2017. Hydrochemical mercury distribution and air-sea exchange over the submarine hydrothermal vents off-shore Panarea Island (Aeolian arc, Tyrrhenian Sea). Mar. Chem. 194, 63–78.
Barde-Cabusson, S., et al., 2009. New geological insights and structural control on fluid circulation in La Fossa cone (Vulcano, Aeolian Islands, Italy). J. Volcanol. Geotherm. Res. 185 (3), 231–245.
Barnes, H., Seward, T., 1997. Geothermal Systems and Mercury Deposits Chapter 14. In: Geochemistry of Hydrothermal Ore Deposits, 3rd ed. Wiley.
Berger, B.R., Eimon, P.I., 1983. Conceptual models of epithermal metal deposits. In: Shanks, W.C. (Ed.), Cameron Volume on Unconventional Mineral Depositss. Society of Mining Engineer, New York, pp. 191–205.
Bloom, N.S., Preus, E., Katon, J., Hiltner, M., 2003. Selective extractions to assess the biogeochemically relevant fractionation of inorganic mercury in sediments and soils. Anal. Chim. Acta 479 (2), 233–248.
Boatta, F., et al., 2013. Geochemical survey of Levante Bay, Vulcano Island (Italy), a natural laboratory for the study of ocean acidification. Mar. Pollut. Bull. 73 (2), 485–494.
Bolognesi, L., D'Amore, F., 1993. Isotopic variation of the hydrothermal system on Vulcano Island, Italy. Geochim. Cosmochim. Acta 57 (9), 2069–2082.
Brombach, C.-C., Pichler, T., 2019. Determination of ultra-low volatile mercury concentrations in sulfur-rich gases and liquids. Talanta 199, 277–284.
Brombach, C.-C., et al., 2015. Direct online HPLC-CV-AFS method for traces of methylmercury without derivatisation: a matrix-independent method for urine, sediment and biological tissue samples. Anal. Bioanal. Chem. 407 (3), 973–981.
Capaccioni, B., Tassi, F., Vaselli, O., 2001. Organic and inorganic geochemistry of low temperature gas discharges at the Baia di Levante beach, Vulcano Island, Italy. J. Volcanol. Geotherm. Res. 108 (1), 173–185.
Chiodini, G., Cioni, R., Marini, L., Panichi, C., 1995. Origin of the fumarolic fluids of Vulcano Island, Italy and implications for volcanic surveillance. Bull. Volcanol. 57 (2), 99–110.
Clever, H.L., Johnson, S.A., Derrick, M.E., 1985. The solubility of mercury and some sparingly soluble mercury salts in water and aqueous electrolyte solutions. J. Phys. Chem. Ref. Data 14 (3), 631–680.
Cossa, D., Martin, J.-M., Takayanagi, K., Sanjuan, J., 1997a. The distribution and cycling of mercury species in the western Mediterranean. Deep-Sea Res. II Top. Stud. Oceanogr. 44 (3), 721–740.
Cossa, D., Martin, J.M., Takayanagi, K., Sanjuan, J., 1997b. The distribution and cycling of mercury species in the western Mediterranean. Deep-Sea Res. Part Ii-Topical Stud. Oceanography 44 (3–4), 721–740.
Cossa, D., et al., 2011. Mercury in the Southern Ocean. Geochim. Cosmochim. Acta 75 (14), 4037–4052.
Cossa, D., et al., 2018. Sources and exchanges of mercury in the waters of the northwestern Mediterranean margin. Prog. Oceanogr. 163, 172–183.
Davey, H.A., van Moort, J.C., 1986. Current mercury deposition at Ngawha Springs, New Zealand. Appl. Geochem. 1 (1), 75–93.
De Astis, G., La Volpe, L., Peccerillo, A., Civetta, L., 1997. Volcanological and petrological evolution of Vulcano island (Aeolian Arc, southern Tyrrhenian Sea). J. Geophys. Res. Solid Earth 102 (B4), 8021–8050.
Di Liberto, V., Nuccio, P.M., Paonita, A., 2002. Genesis of chlorine and Sulphur in fumarolic emissions at Vulcano Island (Italy): assessment of pH and redox conditions in the hydrothermal system. J. Volcanol. Geotherm. Res. 116 (1), 137–150.
Esposito, V., et al., 2018. Exceptional discovery of a shallow-water hydrothermal site in the SW area of Basiluzzo islet (Aeolian archipelago, South Tyrrhenian Sea): an environment to preserve. PLoS One 13 (1), e0190710.
Falcone, E.E., Federico, C., Boudoire, G., 2022. Geochemistry of trace metals and Rare Earth Elements in shallow marine water affected by hydrothermal fluids at Vulcano (Aeolian Islands, Italy). Chem. Geol. 593, 120756.
Federico, C., Capasso, G., Paonita, A., Favara, R., 2010. Effects of steam-heating processes on a stratified volcanic aquifer: stable isotopes and dissolved gases in thermal waters of Vulcano Island (Aeolian archipelago). J. Volcanol. Geotherm. Res. 192 (3), 178–190.
Ferrara, R., Mazzolai, B., Lanzillotta, E., Nucaro, E., Pirrone, N., 2000. Volcanoes as emission sources of atmospheric mercury in the Mediterranean basin. Sci. Total Environ. 259 (1), 115–121.
Fitzgerald, W.F., Lamborg, C.H., Hammerschmidt, C.R., 2007. Marine biogeochemical cycling of mercury. Chem. Rev. 107 (2), 641–662.
Fulignati, P., Gioncada, A., Sbrana, A., 1998. Geologic model of the magmatichydrothermal system of vulcano (Aeolian Islands, Italy). Mineral. Petrol. 62 (3–4), 195–222.
Gamo, T., Glasby, G.P., 2003. Submarine hydorthermal activity in coastal zones. Land Marine Hydrogeol. 151–163.
Horvat, M., et al., 2003. Speciation of mercury in surface and deep-sea waters in the Mediterranean Sea. Atmos. Environ. 37, 93–108.

Hsu-Kim, H., Kucharzyk, K.H., Zhang, T., Deshusses, M.A., 2013. Mechanisms regulating mercury bioavailability for Methylating microorganisms in the aquatic environment: a critical review. Environ. Sci. Technol. 47 (6), 2441–2456.
Inguaggiato, S., et al., 2012. Total CO2 output from Vulcano island (Aeolian Islands, Italy). Geochem. Geophys. Geosyst. 13 (2).
Johnson, A., Cronan, D.S., 2001. Hydrothermal metalliferous sediments and waters off the Lesser Antilles. Marine Geosources Geotechnol. 19 (2), 65–83.
Keller, J., 1980. The island of Vulcano. Rend. Soc. Ital. Mineral. Petrol. 36, 369–414.
Khimasia, A., Renshaw, C., Price, R.E., Pichler, T., 2021. Hydrothermal flux and porewater geochemistry in Paleochori Bay, Milos, Greece. Chem. Geol. 571, 120188.
King, S.A., et al., 2006. Mercury in water and biomass of microbial communities in hot springs of Yellowstone National Park, USA. Appl. Geochem. 21 (11), 1868–1879.
Kotnik, J., Sprovieri, F., Ogrinc, N., Horvat, M., Pirrone, N., 2014. Mercury in the Mediterranean, part I: spatial and temporal trends. Environ. Sci. Pollut. Res. 21 (6), 4063–4080.
Kuss, J., Holzmann, J., Ludwig, R., 2009. An elemental mercury diffusion coefficient for natural waters determined by molecular dynamics simulation. Environ. Sci. Technol. 43 (9), 3183–3186.
Lalonde, J.D., Amyot, M., Kraepiel, A.M.L., Morel, F.M.M., 2001. Photooxidation of Hg (0) in artificial and natural waters. Environ. Sci. Technol. 35 (7), 1367–1372.
Lamborg, C.H., Fitzgerald, W.F., O'Donnell, J., Torgersen, T., 2002. A non-steady-state compartmental model of global-scale mercury biogeochemistry with interhemispheric atmospheric gradients. Geochim. Cosmochim. Acta 66 (7), 1105–1118.
Leal-Acosta, M.L., Shumilin, E., Mirlean, N., Sapozhnikov, D., Gordeev, V., 2010. Arsenic and mercury contamination of sediments of geothermal springs, mangrove lagoon and the Santispac bight, Bahia Concepcion, Baja California peninsula. Bull. Environ. Contam. Toxicol. 85 (6), 609–613.
Leal-Acosta, M.L., Shumilin, E., Mirlean, N., Delgadillo-Hinojosa, F., Sánchez-Rodríguez, I., 2013. The impact of marine shallow-water hydrothermal venting on arsenic and mercury accumulation by seaweed Sargassum sinicola in Concepcion Bay, Gulf of California. Environ Sci Process Impacts 15 (2), 470–477.
Leal-Acosta, M.L., et al., 2018. Intertidal geothermal hot springs as a source of trace elements to the coastal zone: a case study from Bahia Concepcion, Gulf of California. Mar. Pollut. Bull. 128, 51–64.
Lehnherr, I., St. Louis, V.L., Hintelmann, H., Kirk, J.L., 2011. Methylation of inorganic mercury in polar marine waters. Nat. Geosci. 4 (5), 298–302.
Liss, P.S., Slater, P.G., 1974. Flux of gases across the Air-Sea Interface. Nature 247 (5438), 181–184.
Madonia, P., Capasso, G., Favara, R., Francofonte, S., Tommasi, P., 2015. Spatial distribution of field Physico-chemical parameters in the Vulcano Island (Italy) coastal aquifer: Volcanological and hydrogeological implications. Water 7 (7), 3206–3224.
Mason, R., Fitzgerald, W., 1996. Sources, sinks and biogeochemical cycling of mercury in the ocean, Global and regional mercury cycles: sources, fluxes and mass balances. Springer, pp. 249–272.
Mason, R.P., Sheu, G.R., 2002. Role of the ocean in the global mercury cycle. Glob. Biogeochem. Cycles 16 (4), 1093.
McCarthy, K.T., Pichler, T., Price, R.E., 2005. Geochemistry of champagne Hot Springs shallow hydrothermal vent field and associated sediments, Dominica, Lesser Antilles. Chem. Geol. 224, 55–68.
McGinnis, D.F., et al., 2011. Discovery of a natural CO2 seep in the German North Sea: implications for shallow dissolved gas and seep detection. J. Geophys. Res. Oceans 116 (C3).
Monperrus, M., et al., 2007. Mercury methylation, demethylation and reduction rates in coastal and marine surface waters of the Mediterranean Sea. Mar. Chem. 107 (1), 49–63.
Munson, K.M., Lamborg, C.H., Boiteau, R.M., Saito, M.A., 2018. Dynamic mercury methylation and demethylation in oligotrophic marine water. Biogeosciences 15 (21), 6451–6460.
Nicholson, K., 1993. Geothermal Fluids Chemistry & Exploration Technique. Springer Verlag. Inc, Berlin.
Nuccio, P.M., Paonita, A., Sortino, F., 1999. Geochemical modeling of mixing between magmatic and hydrothermal gases: the case of Vulcano Island, Italy. Earth Planet. Sci. Lett. 167, 321–333.
Oliveri, Y., Cangemi, M., Capasso, G., Saiano, F., 2019. Pathways and fate of REE in the shallow hydrothermal aquifer of Vulcano island (Italy). Chem. Geol. 512, 121–129.
Outridge, P.M., Mason, R.P., Wang, F., Guerrero, S., Heimburger-Boavida, L.E., 2018. Updated global and oceanic mercury budgets for the United Nations global mercury assessment 2018. Environ. Sci. Technol. 52 (20), 11466–11477.
Paonita, A., Favara, R., Nuccio, P.M., Sortino, F., 2002. Genesis of fumarolic emissions as inferred by isotope mass balances: CO2 and water at Vulcano Island, Italy. Geochim. Cosmochim. Acta 66 (5), 759–772.
Pichler, T., Veizer, J., 2004. The precipitation of aragonite from shallow-water hydrothermal fluids in a coral reef, Tutum Bay, Ambitle Island, Papua New Guinea. Chem. Geol. 207 (1–2), 31–45.
Pichler, T., Giggenbach, W.F., McInnes, B.I.A., Buhl, D., Duck, B., 1999a. Fe-sulfide formation due to seawater-gas-sediment interaction in a shallow water hydrothermal system at Lihir Island, Papua New Guinea. Econ. Geol. 94, 281–288.
Pichler, T., Veizer, J., Hall, G.E.M., 1999b. The chemical composition of shallow-water hydrothermal fluids in Tutum Bay, Ambitle Island, Papua New Guinea and their effect on ambient seawater. Mar. Chem. 64 (3), 229–252.
Pichler, T., Veizer, J., Hall, G.E.M., 1999c. Natural input of arsenic into a coral-reef ecosystem by hydrothermal fluids and its removal by Fe(III) oxyhydroxides. Environ. Sci. Technol. 33 (9), 1373–1378.
Pichler, T., et al., 2019. Suitability of the shallow water hydrothermal system at Ambitle Island (Papua New Guinea) to study the effect of high pCO2 on coral reefs. Mar. Pollut. Bull. 138, 148–158.
Price, R.E., Giovannelli, D., 2017. A Review of the Geochemistry and Microbiology of Marine Shallow-Water Hyrothermal Vents. Reference Module in Earth Systems and Environmental Sciences.
Price, R.E., Pichler, T., 2005. Distribution, speciation and bioavailability of arsenic in a shallow-water submarine hydrothermal system, Tutum Bay, Ambitle Island, PNG. Chem. Geol. 224, 122–135.
Price, R.E., et al., 2013a. Processes influencing extreme As enrichment in shallow-sea hydrothermal fluids of Milos Island, Greece. Chem. Geol. 348, 15–26.
Price, R.E., et al., 2013b. Archaeal and bacterial diversity in an arsenic-rich shallow-sea hydrothermal system undergoing phase separation. Front. Microbiol. 4 (158), 1–19.
Prol-Ledesma, R.M., Canet, C., Torres-Vera, M.A., Forrest, M.J., Armienta, M.A., 2004. Vent fluid chemistry in Bahia Concepcion coastal submarine hydrothermal system, Baja California Sur, Mexico. J. Volcanol. Geotherm. Res. 137, 311–328.
Roberts, H., Price, R., Brombach, C.-C., Pichler, T., 2021. Mercury in the hydrothermal fluids and gases in Paleochori Bay, Milos, Greece. Mar. Chem. 233, 103984.
Rogers, K.L., Amend, J.P., Gurrieri, S., 2007. Temporal changes in fluid chemistry and energy profiles in the Vulcano Island hydrothermal system. Astrobiology 7 (6), 905–932.
Saunders, J.A., Brueseke, M.E., 2012. Volatility of se and Te during subduction-related distillation and the geochemistry of epithermal ores of the western United States. Econ. Geol. 107 (1), 165–172.
Saunders, J.A., et al., 2008. Genesis of middle Miocene Yellowstone hotspot-related bonanza epithermal Au–Ag deposits, northern Great Basin, USA. Mineral. Deposita 43 (7), 715–734.
Sedwick, P., Stuben, D., 1996. Chemistry of shallow submarine warm springs in an arc-volcanic setting: Vulcano Island, Aeolian archipelago, Italy. Mar. Chem. 53 (1–2), 147–161.
Sommaruga, C., 1984. Le ricerche geotermiche svolte a Vulcano negli anni'50. Rend. Soc. Ital. Mineral. Petrol. 39 (2), 355–366.
Stoffers, P., et al., 1999. Elemental mercury at submarine hydrothermal vents in the Bay of Plenty, Taupo volcanic zone, New Zealand. Geology 27 (10), 931–934.
USEPA, 2002. In: Water, O.O. (Ed.), Method 1631, Revision E: Mercury in Water by Oxidation, Purge and Trap, and Cold Vapor Atomic Fluorescence Spectrometry.
Valsami-Jones, E., et al., 2005. The geochemistry of fluids from an active shallow submarine hydrothermal system: Milos island, Hellenic Volcanic Arc. J. Volcanol. Geotherm. Res. 148 (1–2), 130–151.
Varekamp, J.C., Buseck, P.R., 1984. The speciation of mercury in hydrothermal systems, with applications to ore deposition. Geochim. Cosmochim. Acta 48 (1), 177–185.
Wang, Y.M., et al., 2015. Elemental mercury in natural waters: occurrence and determination of particulate Hg(0). Environ. Sci. Technol. 49 (16), 9742–9749.
Wängberg, I., et al., 2001. Estimates of air-sea exchange of mercury in the Baltic Sea. Atmos. Environ. 35 (32), 5477–5484.
Wanninkhof, R., 1992. Relationship between wind speed and gas exchange over the ocean. J. Geophys. Res. Oceans 97 (C5), 7373–7382.
Williams-Jones, A.E., Heinrich, C.A., 2005. 100th anniversary special paper: vapor transport of metals and the formation of magmatic-hydrothermal ore deposits. Econ. Geol. 100 (7), 1287–1312.
Zambardi, T., Sonke, J.E., Toutain, J.P., Sortino, F., Shinohara, H., 2009. Mercury emissions and stable isotopic compositions at Vulcano Island (Italy). Earth Planet. Sci. Lett. 277 (1), 236–243.
Zhao, L., et al., 2016. Evolution of bubble size distribution from gas blowout in shallow water. J. Geophys. Res. Oceans 121 (3), 1573–1599.